The Nelson Mandela African Institution of Science and Technology

http://dspace.nm-aist.ac.tz

Materials, Energy, Water and Environmental Sciences   Research Articles [MEWES]

2019-11-23

A Novel and Facile Method to Characterize the Suitability of Metallic Iron for Water Treatment

Lufingo, Mesia

MDPI

A Novel and Facile Method to Characterize the Suitability of Metallic Iron for Water Treatment

Mesia Lufingo [1,*] , **Arnaud Igor Ndé-Tchoupé** [2] , **Rui Hu** [3] , **Karoli N. Njau** [1] **and**
Chicgoua Noubactep [3,4,*]

[1] Department of Water and Environmental Science and Engineering, Nelson Mandela African Institution of Science and Technology, Arusha 23311, Tanzania; karoli.njau@nm-aist.ac.tz

[2] Department of Chemistry, Faculty of Sciences, University of Douala, Douala B.P. 24157, Cameroon; ndetchoupe@gmail.com

[3] School of Earth Science and Engineering, Hohai University, Fo Cheng Xi Road 8, Nanjing 211100, China; rhu@hhu.edu.cn

[4] Department of Applied Geology, Universität Göttingen, Goldschmidtstraße 3, D-37077 Göttingen, Germany

* Correspondence: lufingom@nm-aist.ac.tz (M.L.); cnoubac@gwdg.de (C.N.); Tel.: +255-755-142-521 (M.L.); +49-551-393-3191 (C.N.)

Abstract: Metallic iron (Fe^0) materials have been industrially used for water treatment since the 1850s. There are still many fundamental challenges in affordably and reliably characterizing the Fe^0 intrinsic reactivity. From the available methods, the one using Fe^0 dissolution in ethylenediaminetetraacetic acid (EDTA—2 mM) was demonstrated the most applicable as it uses only four affordable chemicals: Ascorbic acid, an ascorbate salt, EDTA and 1,10-Phenanthroline (Phen). A careful look at these chemicals reveals that EDTA and Phen are complexing agents for dissolved iron species. Fe^3-EDTA is very stable and difficult to destabilize; ascorbic acid is one of the few appropriate reducing agents, therefore. On the other hand, the Fe^2-Phen complex is so stable that oxidation by dissolved O_2 is not possible. This article positively tests Fe^0 (0.1 g) dissolution in 2 mM Phen (50 mL) as a characterization tool for the intrinsic reactivity, using 9 commercial steel wool (Fe^0 SW) specimens as probe materials. The results are compared with those obtained by the EDTA method. The apparent iron dissolution rate in EDTA (k_{EDTA}) and in Phen (k_{Phen}) were such that $0.53 \leq k_{EDTA}$ ($\mu g\ h^{-1}$) ≤ 4.81 and $0.07 \leq k_{Phen}$ ($\mu g\ h^{-1}$) ≤ 1.30. Higher k_{EDTA} values, relative to k_{Phen}, are a reflection of disturbing Fe^3 species originating from Fe^2 oxidation by dissolved O_2 and dissolution of iron corrosion products. It appears that the Phen method considers only the forward dissolution of Fe^0. The Phen method is reliable and represents the most affordable approach for characterizing the suitability of Fe^0 for water treatment.

Keywords: 1,10-Phenanthroline; ethylenediaminetetraacetic acid; intrinsic reactivity; water treatment; zero-valent iron

1. Introduction

Inadequate access to safe drinking water (and sanitation) is the most pervasive problem currently afflicting the developing world [1–6]. Moreover, water scarcity is expected to grow worse in the coming decades, even in regions currently considered water-rich [1,7]. Therefore, new robust, efficient, affordable, and applicable water treatment technologies are urgently needed [1,7,8]. Ideally, such innovative technologies should be simple to operate and maintain, be able to function without electricity and be based on local resources and skills [2,4,5]. Filtration on metallic iron (Fe^0) beds has been discussed in the literature as such an applicable technology for universal access to safe drinking water to low-income communities [9,10].

The design, construction, and management of Fe^0-based filtration systems is a typical civil engineering task. The management comprises filter maintenance, waste disposal, and Fe^0 recycling [2,11–13]. Such projects can be made sustainable and large scale applicable by science-basing the design [8,12,14–16]. This design should consider the Fe^0 life cycle as Fe^0 is the 'heart' of the system. Characterizing the Fe^0 life cycle [17] starts and ends with carefully characterizing (1) the intrinsic reactivity of each used material, (2) its time-dependent corrosion kinetic, and (3) the impact of its corrosion products (FeCPs) on the hydraulic conductivity (permeability loss) of the designed filter [18]. Although all three aspects are known from the mainstream iron corrosion literature, available knowledge has not yet been summarized to enable a science-based design of Fe^0-based filters [10,12,15,18,19]. The present work is focused on characterizing the Fe^0 intrinsic reactivity. It is just recalled here that (1) each Fe^0 specimen has its own intrinsic reactivity [20–22], (2) the time-dependent corrosion kinetic of Fe^0 corrosion is best described in investigations for modeling the cracking of reinforced concrete structures [23–25] and (3) the volumetric expansive nature of iron corrosion [26] is the first cause of permeability loss in Fe^0-based filters [14,27–30].

Information regarding the Fe^0 intrinsic reactivity is largely confusing because 'reactivity' and 'efficiency' are often randomly interchanged [12,15,31,32]. A representative example is a recent article by [33] entitled "Enhanced reactivity and electron selectivity of sulfidated Fe^0 toward chromate under aerobic conditions", wherein the authors comparatively presented results of Cr^6 removal in the Fe^0/H_2O versus $S-Fe^0/H_2O$ systems. $S-Fe^0$ is a sulfidated specimen, a Fe^0/S composite. For each Fe^0 specimen, the $S-Fe^0/H_2O$ system was more efficient at removing Cr^6 than the Fe^0/H_2O system: 7.5- and 10.7-fold greater removal efficient [33]. This good experimental observation was interpreted by considering an increase of the Fe^0 specific surface area (aspect 1) because of the enrichment of Cr^6 anions in the FeS_x layer. Additionally, the FeS_x layer (shielding Fe^0) is anion-selective (aspect 2). Both aspects (1 and 2) were reported to favor 'selective' electron transfer from the Fe^0 core to Cr^6 because FeS_x is electronic conductive. While this interpretation is accepted, it has not out ruled alternative views. For example, (1) sulfidation increases electron mobility in the composite, and thus the intrinsic reactivity, (2) Fe^0 is corroded by water to produce Fe^2 (and H_2), and Cr^6 is reduced by Fe^2 [34–36]. Additionally, the Fe^0 surface is permanently shielded by a positively charged oxide-scale [37–41] attracting Cr^6 anions. The evidence that alloying with S (sulfidation) enhances the intrinsic reactivity of each Fe^0 should not be misinterpreted as "sulfidation improves the Fe^0 efficiency" because designing an efficient system is a site-specific task. For example, if a more reactive material is unnecessarily used at a given site, rapid system clogging will be the net result: Initially efficient but not sustainable [2].

Reliable information about the intrinsic reactivity of Fe^0 materials is crucial in designing efficient and sustainable Fe^0-based filters [9,18,20,22,42–49]. Li et al. [22] recently reviewed information about appropriately selecting Fe^0 materials for water treatment and environmental remediation. They presented an extensive overview of available tools to characterize Fe^0 materials including the determination of the specific surface area, the in situ characterization of corrosion processes and the characterization of Fe^0 morphology and size. They highlighted that, because of the complexity of the Fe^0/H_2O system and the uniqueness of each Fe^0 specimen, different characterization tools should be employed together to facilitate the deployment of the next generation sustainable Fe^0-based remediation systems. This statement is in tune with efforts that have culminated in the use of ethylenediaminetetraacetic acid (EDTA) to characterize the Fe^0 intrinsic reactivity some 15 years ago [45].

The present work is a continuation of an effort to characterize the intrinsic reactivity of Fe^0 specimens based on the kinetics of their dissolution in a dilute solution of complexing agents. Previous works were based on Fe^0 dissolution in EDTA [9,20,21,45,50,51]. The interpretation of achieved results was complicated by the evidence that EDTA dissolves amorphous Fe^3-components of iron corrosion products (FeCPs) as well [51,52]. This is due to the extreme stability of the Fe^3-EDTA complex [53–56]. Therefore, characterizing the intrinsic reactivity of very reactive Fe^0 material such as steel wool specimens (Fe^0 SW) was very challenging [51]. In other words, developing a tool to reliably characterize the intrinsic reactivity of Fe^0 SW would be a progress for the Fe^0 remediation community.

The purpose of this study was to develop an experimental method to characterize the intrinsic reactivity of Fe^0 SW using their initial dissolution in 1,10-Phenanthroline (ortho-Phenanthroline or Phen). Nine (9) commercial Fe^0 SW were used. The selection of Phen was justified by the extreme stability of the Fe^2-Phen complex [53,55]: (1) avoiding any further oxidation of Fe^2 from Fe^0 dissolution and (2) non-addressing any Fe^3 species already available in the system [52]. Parallel experiments using EDTA were performed and the results are comparatively discussed.

2. Materials and Methods

2.1. Solutions

Working solutions were prepared from a monohydrated 1,10-Phenanthroline (Phen) (Merck, Darmstadt, Germany) and a disodium salt of ethylenediaminetetraacetic (EDTA) (Merk, Darmstadt, Germany). An iron standard solution (1000 mgL^{-1}, NIST®(Gaithersburg, MD, USA)) from HACH (Loveland, CO, USA) was used to calibrate the spectrophotometer. Other used chemicals included ascorbic acid, hydrochloric acid, and nitric acid. All used chemicals were of analytical grade.

2.2. Fe^0 Materials

A total of nine (9) locally available commercial steel wool (Fe^0 SW) specimens were purchased from East Africa Steel Wool (Ind.) Limited in Dar Es Salaam (Tanzania) and used. The tested 9 Fe^0 SW covered all grades of steel wools. Table 1 summarizes the main characteristics of the materials together with their elemental composition.

Table 1. Major characteristics of tested metallic iron (Fe^0) steel wool (SW) specimens. The elemental composition (%) was determined in this study. SW1 to SW8 originated from China and SW9 from Tanzania. SW1 to SW8 were brand new, direct from the manufacturer, while SW9 was bought on the market in Tengeru (Tanzania). SW9 was thus air oxidized to some extent. The n.d. stands for not detected.

Material Code	Diameter (mm)	Grade Number	Name	Elemental Composition					
				Fe	Co	Cu	Pb	Ni	Cr
SW1	0.025	0000	Super Fine	99.15	0.01	0.03	0.40	0.09	0.32
SW2	0.035	000	Extra Fine	99.21	0.05	0.12	n.d.	0.16	0.47
SW3	0.04	00	Very Fine	99.25	0.05	0.16	n.d.	0.11	0.43
SW4	0.05	0	Fine	99.08	0.05	0.27	n.d.	0.11	0.49
SW5	0.06	1	Medium	98.37	0.05	1.00	n.d.	0.11	0.45
SW6	0.075	2	Medium Coarse	99.14	0.04	0.27	n.d.	0.10	0.45
SW7	0.09	3	Coarse	98.69	0.05	0.40	0.40	0.14	0.33
SW8	0.1	4	Extra Coarse	99.27	0.04	0.28	n.d.	0.10	0.30
SW9	0.04	00	Very Fine	99.62	0.01	0.02	n.d.	0.03	0.32

2.3. Experimental Procedure

2.3.1. Elemental Composition of Used Fe^0 SW

The procedure presented by [57] was used. A solution containing HNO_3 (70%), HCl (35%) and de-ionized water was prepared at a 1:1:1 ratio by volume. Analytes were prepared by adding 12 mL of the mixed acid solution to 0.5 g of Fe^0 SW in a beaker. The beaker was covered with a watch glass, and after 10 min pre-digestion at room temperature (23 ± 2 °C), the solution was gradually heated on a hotplate for approximately 30 min to 200 °C. After cooling for about 15 min, the sample digest was made up to 100 mL with de-ionized water, and an aliquot was transferred to a 50 mL auto-sampler vial for analysis. Then, 1 mL of the sample was diluted with de-ionized water to a mark in a 250 mL volumetric flask prior to Inductively Coupled Plasma (ICP) analysis.

2.3.2. Iron Dissolution

Iron dissolution studies were accomplished by using 0.10 g of each Fe^0 SW in 50 mL of the complexing agent (2 mM Phen, 6 mM Phen, and 2 mM EDTA) for up to 5 days (120 h). The experiments were performed with the conventional quiescent experimental protocol for the EDTA test [45]. Tested SW specimens were cut into 2 to 3 cm before weighing and submerged in 50 mL graduated plastic cell-star tubed (narrow beakers) containing EDTA or O-Phen. All experiments were performed in triplicates, protected from direct sunlight.

2.3.3. Analytical Method

The aqueous iron concentration was determined with a Rayleigh UV/VIS Spectrophotometer (Beijing Beifen-Ruili Analytical Instruments (group) Co., Ltd., Beijing, China), at a wavelength of 510 nm using a 1.0 cm cuvette. The instrument was calibrated for iron concentration ≤ 10 mg L^{-1}. An ascorbate buffer was used to reduce Fe^3-EDTA before adding Phen for Fe^2 complexation before Fe determination. Samples from the Phen experiments were treated in the same way as the same calibration curve was used [21].

2.3.4. Expression of Results

The basic idea of using complexing agents to characterize the intrinsic reactivity of Fe^0 materials is that iron dissolution (from Fe^0 and FeCPs) is initially a linear function of the time [45]. Thus, for a certain time frame ($t_1 > t_0$) after the initiation of the experiment (t_0) the total iron concentration ($[Fe]_t$) as defined in Equation (1) is a linear function (of time).

$$[Fe]_t = a \times t + b \tag{1}$$

Therefore, the goal of this study was to identify the time frame for the linearity of Equation (1). The regression coefficients (a and b) are characteristic for each Fe^0 specimen. In fact, "a" is the rate of Fe dissolution from Fe^0 while "b" gives an estimation of the amount of FeCPs on the material or the fraction thereof that is dissolved by the used complexing agent (here EDTA and Phen). For the EDTA and Phen dissolution experiments, the corresponding values are termed as k_{EDTA} and k_{Phen}, respectively. Herein, k_{EDTA} and k_{Phen} values were obtained from Microsoft Excel 2017 (Microsoft, Redmond, WA, USA).

3. Results and Discussion

The results of elemental analysis are presented in Table 1. It is seen that all 9 specimens are made up of at least 98.4 % Fe. Accordingly, differences in intrinsic reactivity are due to the manufacturing process (not accessible) and to the distribution of the remaining 1.4% alloying elements. Relevant elements are Co, Cr, Cu, Ni, and Pb (Table 1). For both Grade 00 specimens (very fine: SW3 and SW9) differences can also be attributed to the surface oxidation state.

3.1. Appropriateness of the Experimental Approach

Figure 1 compares the results of SW9 dissolution in three different solutions: 2 mM EDTA, 2 mM Phen, and 6 mM Phen. EDTA dissolved far more iron than Phen (up to 40 mg L^{-1} vs. less than 8 mg L^{-1}). Furthermore, there was no difference in the extent of iron dissolution in 2 mM and 6 mM Phen. It should be kept in mind that 6 mM Phen (Fe:Phen = 1:3) corresponds to 2 mM EDTA (Fe:EDTA = 1:1) in the stoichiometry of Fe complexation by both agents. The differential behavior from Figure 1 is explained by considering the chemistry of the system. In fact, in both cases, Fe^0 was corroded by water (H_2O or H^+) according to Equation (2).
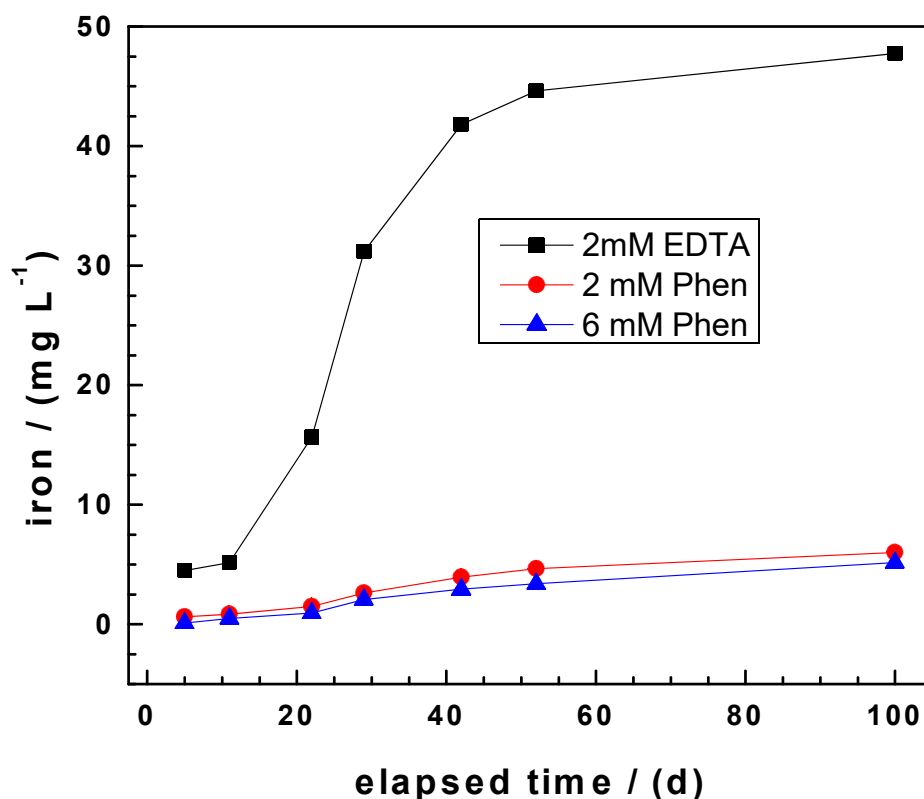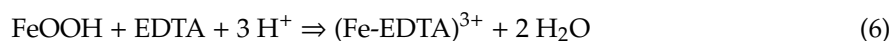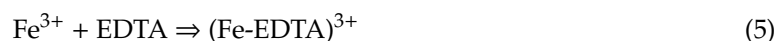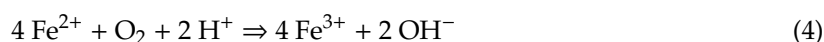
Figure 1. Comparison of the dissolution rate of SW9 in ethylenediaminetetraacetic (EDTA, 2 mM) and 1,10 Phenantroline (Phen, 2 mM; 6 mM) solutions quiescent conditions for 83 h. Experimental conditions: m_{SW} = 0.1 g, $V_{solution}$ = 50 mL. The represented lines are not fitting functions, they just connect the points to ease visualization.

$$Fe^0 + 2\,H^+ \Rightarrow Fe^{2+} + H_2 \tag{2}$$

$$Fe^{2+} + Phen \Rightarrow (Fe\text{-}Phen)^{2+} \tag{3}$$

$$4\,Fe^{2+} + O_2 + 2\,H^+ \Rightarrow 4\,Fe^{3+} + 2\,OH^- \tag{4}$$

$$Fe^{3+} + EDTA \Rightarrow (Fe\text{-}EDTA)^{3+} \tag{5}$$

$$FeOOH + EDTA + 3\,H^+ \Rightarrow (Fe\text{-}EDTA)^{3+} + 2\,H_2O \tag{6}$$

In the presence of Phen, Fe^{2+} is complexed to form very stable Fe-Phen (Equation (3)) which blocks the Fe^{2+} oxidation by dissolved oxygen (Equation (4)). In the presence of EDTA, Fe^{2+} oxidation to Fe^{3+} (Equation (4)) is rather accelerated because $(Fe\text{-}EDTA)^{3+}$ is more stable than $(Fe\text{-}EDTA)^{2+}$ [53,55,58]. Resulting Fe^{3+} is then complexed by EDTA (Equation (5)). It should be recalled that $(Fe\text{-}EDTA)^{3+}$ is not destabilized by many inorganic reducing agents, including hydroxylamine. Hydroxylamine is used in the standard spectrophotometric method to reduce Fe^3 species prior to the formation of the characteristic orange complex of Fe^2-Phen [59]. Lastly, amorphous Fe^3 corrosion products are (at least partly) dissolved in EDTA (Equation (6)). Amorphous Fe^2 corrosion products, if available, would dissolve both in EDTA and Phen [52].

The discussion until now clearly shows that the Phen method was (1) not sensible to dissolved oxygen and (2) less sensible to the presence of atmospheric corrosion products on Fe^0 than the EDTA method. Thus, the Phen method was free from an inherent limitation of the EDTA method making its application for characterizing (1) very reactive materials and (2) fine Fe^0 specimens containing large amounts of atmospheric corrosion products [20,51]. Hildebrandt [51] recently presented an original approach to address the second challenge. This consisted of reducing the mass of Fe^0 SW from 0.1 g to 0.01 g in 50 mL of the EDTA solution. Even then, a linear relationship between the elapsed time and the dissolved iron concentration (Equation (1)) was difficult to obtain [51]. The perfect linearity observed for Phen in Figure 1 confirms that using the Phen method practically only Fe^0 oxidative dissolution was characterized [60]. Hu et al. [52] recently presented the first application of the Phen test for granular Fe^0 materials.

3.2. Evidencing the Non-Linear Kinetic of Iron Corrosion

Figure 2 compares changes of iron concentration as a function of time for the 9 tested Fe^0 SW in 2 mM Phen for up to 120 h. For all materials, Fe values increased progressively with the experimental duration, even after 120 h of contact. However, a linear increase was observed only during the first 24 h (1 day). In the Fe^0/Phen/H_2O system, there is no (porous) oxide scale which could justify slow mass transfer into the bulk solution. The solution was also not saturated (Section 3.1). Hence, at longer experimental times, the data indicated the occurrence of a chemical reaction that was slow and specific to each Fe^0 SW specimen. This is the first time that the differential kinetics of Fe^0 oxidative dissolution was clear evidence in short-term quiescent batch experiments.
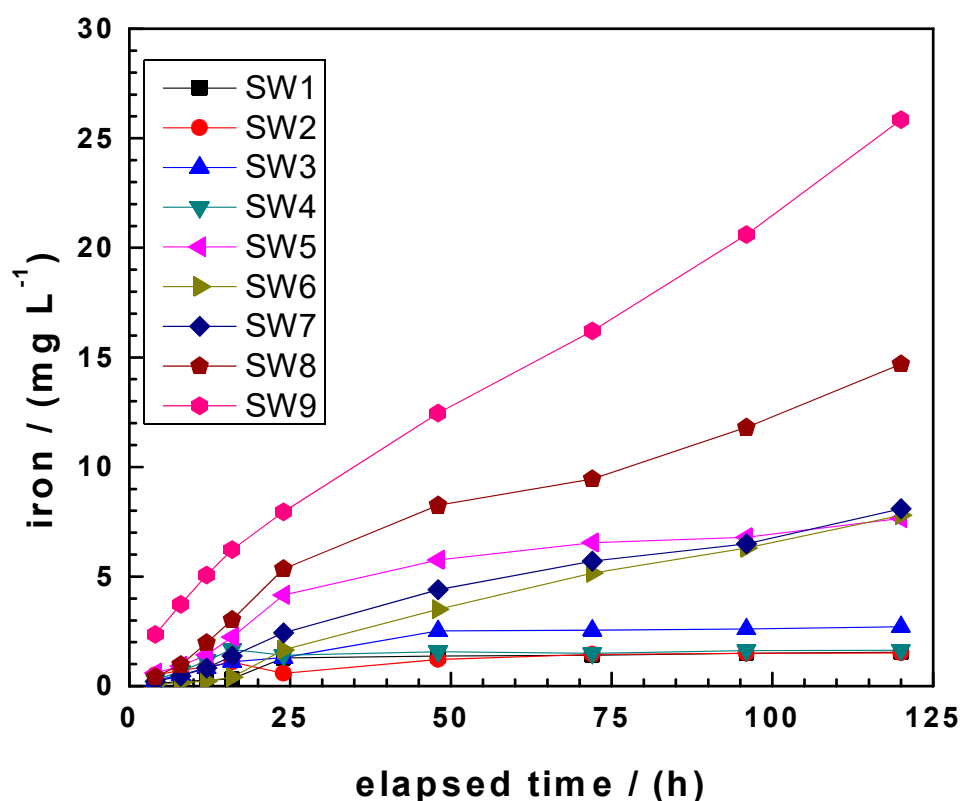

Figure 2. Comparison of the dissolution rate of the tested Fe^0 SW specimens in 1,10 Phenantroline (Phen) under quiescent conditions for 120 h. Experimental conditions: m_{SW} = 0.10 g, [Phen] = 2 mM, $V_{solution}$ = 50 mL. The represented lines are not fitting functions; they just connect the points to ease visualization.

Compared to granular Fe^0 used in EDTA tests [20], filamentous Fe^0 SW was more reactive, but the same mass (0.1 g) could not achieve iron saturation (112 mg L^{-1}). It is recalled that the EDTA test

was stopped after 4 days because saturation was approached for more reactive granular samples [45]. As discussed above, dissolution of atmospheric corrosion products also occurred in EDTA. The data in Figure 2 show that the most reactive Fe^0 SW used herein could not dissolve 30 mg L^{-1} of iron in 2 mM Phen after 120 days. The reason has been that only the slow forward dissolution of Fe^0 was addressed. This evidence makes the Phen test more reliable that the EDTA test. In addition to using fewer chemicals than the EDTA test, the Phen test was also more affordable [52,60].

In a purely analytical perspective, it is recalled that samples from the Phen test, despite already depicting the orange coloration of Fe-Phen complexes, should be treated in the same way like the calibration standards. In this study ascorbic acid was used because of parallel experiments with EDTA [21]. In routine Phen tests, all other reducing agents (e.g., hydroxylamine) can be used, but the authors recommend ascorbic acid for its less toxicity and even its better affordability [59].

3.3. Comparing k_{EDTA} and k_{Phen} Values

Figure 3 summarizes the results of iron dissolution in EDTA (Figure 3a) and Phen (Figure 3b) for 16 h. Figure 3a depicts a large variability of the standard deviation (results not shown) which results from various amounts of atmospheric corrosion products initially available on the SW specimens and the evidence that dissolved O_2 accelerates iron dissolution. For the experiments with Phen (Figure 3b), no such variability was observed as the Phen test is neither sensible to Fe^3 species nor to dissolved O_2 (Section 3.1). Calculations showed that 2 to 16 times more iron was dissolved in the EDTA systems than in the corresponding Phen systems. Extending the experimental duration to 120 h (5 days) revealed differential behaviors for individual Fe^0 SW specimens (Section 3.2, Figure 2). The general trend is that iron dissolution from the coarsest material (SW8) was progressive through the end of the experiments (Figure 2). This trend was also observed for SW9, which was the most reactive by virtue of its "pre-oxidized" surface state.
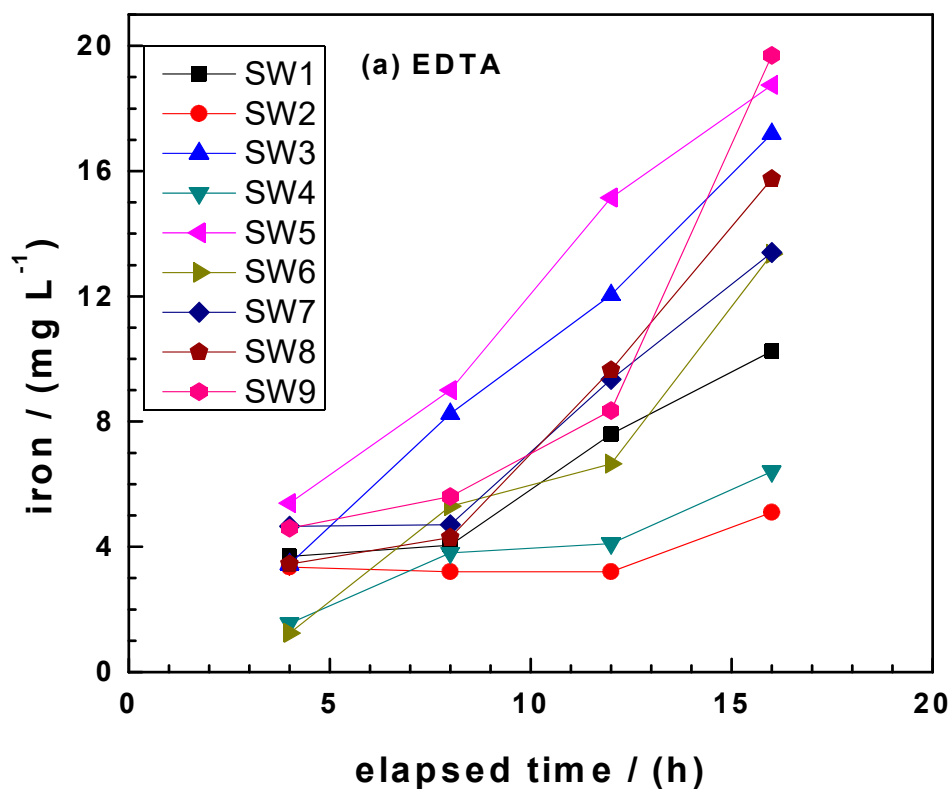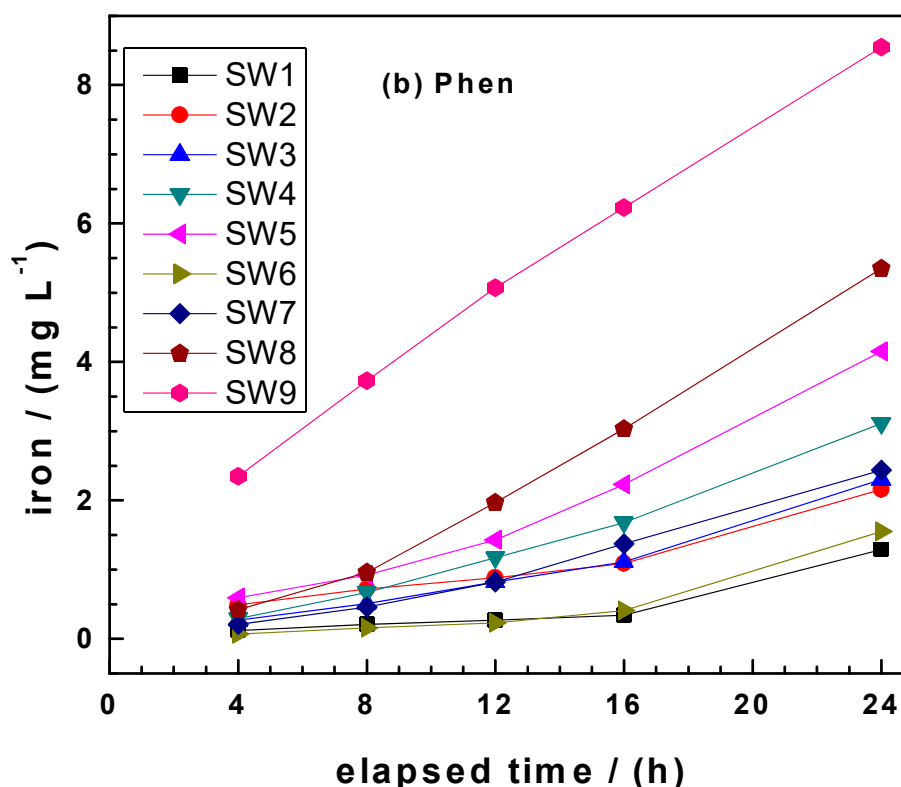

Figure 3. *Cont.*

Figure 3. Comparison of the dissolution rate of the tested Fe[0] SW specimens in (**a**) ethylenediaminetetraacetic (EDTA) and (**b**) 1,10 Phenantroline (Phen) under quiescent conditions for 24 h. Experimental conditions: m_{iron} = 0.10 g, [EDTA] = [Phen] = 2 mM, $V_{solution}$ = 50 mL. The represented lines are not fitting functions; they just connect the points to ease visualization. The regression parameters are listed in Table 2.

Table 2. Corresponding correlation parameters (iron dissolution rate in EDTA (k_{EDTA}) and in Phen (k_{Phen}), b, R^2) for the tested Fe[0] SW specimens. As a rule, the more reactive a material is under given conditions, the larger the k value is. Experimental conditions: [EDTA] = [Phen] = 2 mM, room temperature 23 ± 2 °C, [Fe[0]] = 0.10 g, and $V_{solution}$ = 50 mL. The k_{EDTA}, k_{Phen}, and b values were calculated using Microsoft Excel 2017.

Sample	EDTA				O-Phen			
	k_{EDTA} ($\mu g\ h^{-1}$)	b (mg)	N (-)	R^2 (-)	k_{Phen} ($\mu g\ h^{-1}$)	b (mg)	N (-)	R^2 (-)
SW1	2.320	0.600	5	0.9256	0.072	0.055	5	0.9931
SW2	0.525	2.400	5	0.5338	0.1960	0.3050	5	0.9957
SW3	4.505	(-)1.025	5	0.997	0.2830	(-) 0.03	5	0.9974
SW4	1.385	0.250	5	0.7809	0.4670	(-) 0.215	5	0.9956
SW5	4.620	0.525	5	0.988	0.5430	(-) 0.065	5	0.9635
SW6	3.765	(-)2.775	5	0.9342	0.1090	(-) 0.055	5	0.9539
SW7	3.090	0.300	5	0.8992	0.3840	(-) 0.245	5	0.9700
SW8	4.225	(-)2.275	5	0.9216	0.8840	(-) 0.615	5	0.9808
SW9	4.805	(-)2.45	5	0.7985	1.2980	1.1000	5	0.9984

Table 2 summarizes the k values for both tests for 5 experimental points (N = 5) and an experimental duration of 24 h, corresponding to linearity. The 'a' and R^2 values are also given. The R^2 values for EDTA vary between 0.534 for SW2 and 0.994 for SW3. For Phen all R^2 values were larger than 0.94, confirming the better suitability of the Phen test as already discussed (see also [52]). As concerning the 'b' values, it is seen that for the EDTA test, four from nine values are negative and large in absolute values

(b > 1.03 mg). For the Phen test, only three values are positive but all low (0.055, 0.312, and 1.100 mg), while the 6 negative numbers are very low, (< 0.6 mg). The negative 'b' values from the Phen test were due to the very slow kinetics for iron dissolution from less reactive samples (Figure 3b) while negative value from EDTA test was attributed to dissolved O_2 and atmospheric corrosion products [20,21,52]. The most important parameters from these tests are the k values.

The k values from Table 2 enable a better classification of the order of reactivity of the tested SW specimens. In 2 mM EDTA and Phen, the increasing order of reactivity are:

1.　　EDTA: SW2 < SW4 < SW1 < SW7 < SW6 < SW8 < SW3 < SW5 < SW9.
2.　　Phen: SW1 < SW6 < SW2 < SW3 < SW7 < SW4 < SW5 < SW8 < SW9.

In both cases, SW9 was the most reactive, while SW1 and SW6 were the least reactive (Figures 2 and 3). While the results from the Phen test are more reliable (forward iron dissolution), more research is needed to ascertain whether in the long term the specimens depicting very similar reactivity herein could be differentiated. One curious observation herein is that it is rather the coarsest sample (SW8) which exhibited the largest k_{Phen} value from the brand new materials. Based on the larger surface area depicted by finer materials, the opposite would have been expected. It is recalled that SW9 was from a different origin and had a pre-oxidized surface.

Certainly, the dynamic process of iron dissolution from concentric layers of Fe^0 atoms making up the SW filaments cannot be linear [61,62]. Effects similar to "case hardening" for food and wood drying will lead to "surface hardened layers" [63–65] leading to differential kinetics/extents of Fe dissolution for different particle size ranges. In other words, the extent of restricted corrosion rates through resulting surface hardened layers will be different for different grades of Fe^0 SW. The results of this research suggest that "case hardening" implies that Fe^0 is easier to dissolve from coarser SW than from finer. However, such a conclusion cannot be drawn without considering the manufacturing and storage processes of the different specimens [20].

Comparing the k_{Phen} values having in mind the elemental composition (Table 1) would suggest, for SW8 and SW9, that the Ni content is essential for the Fe^0 reactivity. Both samples practically only differ in their Ni content: 0.10 for SW8 and 0.03 for SW9. However, such a key conclusion cannot be drawn based on one example. It has to be remembered that the goal of this research is to screen and recommend Fe^0 specimens for further research. On the other hand, designing an efficient Fe^0-based water treatment includes selecting the best material to solve a site-specific problem. This might imply purposefully selecting a low reactive material, able to generate satisfactory amounts of corrosion products to achieve water treatment standards for a long time.

Figure 3b shows, interestingly, that iron dissolution from most SW specimens did not take place immediately upon addition of the Phen solution. Iron quantitative dissolution started after a lag time of up to 6 h. Such a lag time was already documented in the process of nitrate removal in Fe^0/H_2O systems [66,67]. The results herein justified why this was not a typical/general observation. A researcher using SW9 would not necessarily observe a lag time because iron dissolution is comparatively rapid.

3.4. Discussion

The need for applicable methods to (1) assesses the intrinsic reactivity of Fe^0 materials and (2) assure their quality control is inherent to the technology and has been recognized in the very early stage of its recent development (post 1990). Summarizing, the experience of the first decade of research [43] recognized difficulties in correlating parameters that had been individually demonstrated to significantly impact the efficiency of remediation systems using Fe^0. Relevant parameters include chemical composition, cooling history, feedstock's processing, kiln firing atmosphere, specific surface area, surface morphology, and type and amount of oxide coatings. The need to further explore these relationships in future research was expressed. However, this effort was not really continued and the Fe^0 reactivity was mainly characterized using selected Fe^0 specimens and various kinds of pollutants (e.g., Cr^6, methylene blue, nitrate, trichloroethylene) [44,47]. The reactivity of the materials was then

reflected by the rate constants of their degradation. However, possible probing reactants are inherently different in their chemistry and rate constants vary by several orders of magnitude, making achieved results of limited guidance in selecting Fe^0 for the practice [47,49]. Some few pollutant-independent characterization methods have been presented and are summarized below in the chronological order of their publication in the peer-reviewed literature. They are briefly commented.

Reardon [42] presented H_2 evolution at neutral pH values as a tool to characterize the reactivity of iron. Probably due to the large Fe^0 amount needed to quantitatively produce H_2 and the long duration of the experiments, this method has not been considered [21]. Noubactep [68] presented H_2 evolution in HCl (initial pH = 2) as a more rapid mean for the same purpose. This tool was completely ignored, perhaps because of the clear different mechanism of H_2 evolution at pH < 4.0 (compared to the field situation pH > 6.0). Noubactep et al. [45] presented the EDTA method which was independently introduced two years later by Pierce et al. [50]. The EDTA method has been continuously used and revisited by Noubactep and collaborators as summarized in [21,52]. Kim et al. [47] introduced a method to measure the 'reductive power' of Fe^0. A tri-iodide/iodide system (I_3^-/I^-, iodine method) was used for the oxidative dissolution of Fe^0 specimens and the rate constant of I_3^- reduction used to characterize the Fe^0 reactivity. The iodine method has not considered all previous methods, perhaps because it uses a redox reaction. Li et al. [49] introduced a method based on the Fe^3/Fe^0 redox reaction (ferric method), which consists of adding a concentrated Fe^3 solution (up to 3000 mg L^{-1}) to a Fe^0 specimen and quantifying the increase in iron concentration after 4 h. The ferric method seems very simple but ferric iron must be available, and strong dilution must precede iron determination, up to factor 100. Lastly, the Phen method presented in this study uses only one chemical, that is also used in all other methods if the iron is to be determined by spectrophotometry using the 1,10 Phenanthroline method [60]. It is thus not only the simplest but also the most affordable. The Phen test has successfully characterized the intrinsic reactivity of steel wool specimens while using the same mass of material (0.1 g) used for the EDTA test. It is obvious that this test will work for coarser materials. In the meantime, Hu et al. [52] have already validated the Phen test using eight commercial granular materials. The major merit of the Phen test is that it uses the same mass of material (0.1 g) regardless of the size and aggregation state (e.g., filamentous, granular).

The well-established common process implying water decontamination by Fe^0 materials is their oxidative dissolution (corrosion). Whether the contaminant is then adsorbed or chemically transformed (oxidized or reduced), oxidation of Fe^0 to Fe^2 (Equation (2)) is the first step [10,30]. Precisely, this process is characterized by the Phen method and is neither disturbed by dissolved O_2 nor atmospheric FeCPs. Therefore, k_{Phen} values provide a reliable and confident parameter to characterize reactive Fe^0 materials. Following the roadmap of [18], it is time to build a significant k_{Phen} database for available Fe^0 materials to prepare their systematic testing in long-term column experiments. Once a significant number of materials differing in their k_{Phen} values are tested in such long-term experiments, it will be possible to reliably recommend selected ones for the site-specific design of field Fe^0/H_2O systems. In other words, the data provided herein are a clear starting point for the design of future laboratory, pilot, and field-scale studies for the design of the next generation Fe^0 remediation systems to achieve the United Nations Sustainable Development Goals (UN SDGs) [18]. Further work should also use other affordable approaches like the methylene blue method (MB method) [69] to quickly access the impact of various parameters of the system efficiency. The MB method takes advantage of the differential affinity of MB toward sand and iron oxides (FeCPs). Thus, a system containing sand and Fe^0 discolors always lesser MB the more sand is in situ coated by FeCPs.

The results presented herein also clarify the influence of complexing agents (including EDTA and Phen) on the efficiency of Fe^0/H_2O systems. Complexing agents are often used to avoid the precipitation of $Fe(OH)_3$ and, thus, to clarify the mechanisms of contaminant removal in Fe^0/H_2O systems [58,70,71]. Despite 25 years of intensive research, the reaction mechanism is still controversially discussed [72–75]. The present study confirms that both EDTA and Phen avoid iron precipitation before the solution is saturated (e.g., [Fe] > 112 mg L^{-1} for 2 mM EDTA). The results also suggest that (1) contaminant reduction should be quantitative in the presence of both EDTA and Phen because Fe^0

dissolution is accelerated or (2) any observed contaminant reduction in their presence results from Fe^2 oxidation (electrons from Fe^2). Case (2) suggests that contaminant reduction is only observed in the presence of EDTA as Phen blocs Fe^2 oxidation. Exactly, this was observed by [58] investigating aqueous Cr^6 removal as influenced by EDTA, NaF, and Phen. Indirectly, [58] have demonstrated that aqueous Cr^6 is removed only when Fe precipitates. Their observation is thus consistent with the concept that adsorption and co-precipitation are the fundamental mechanisms of contaminant removal in Fe^0/H_2O systems [4,10,73–76].

4. Conclusions

Iron dissolution in 2 mM 1,10-Phenanthroline (Phen test) provides an accurate and reliable method to characterize the intrinsic reactivity of Fe^0 materials for water treatment. The Phen test uses only one reagent, is environmentally friendly, and takes just 16 h. Here, it is conducted with a conventional spectrophotometer in a low-equipped laboratory, and it is thus universally applicable. The Phen test can be further developed to be used to assess the long-term kinetics of iron corrosion to help design sustainable filtration systems. This simple method is ready to serve as a universal testing procedure for Fe^0 suppliers and is a standard candidate procedure for testing Fe^0 materials for environmental applications.

References

1. Shannon, M.A.; Bohn, P.W.; Elimelech, M.; Georgiadis, J.G.; Marinas, B.J.; Mayes, A.M. Science and technology for water purification in the coming decades. *Nature* **2008**, *452*, 301–310. [CrossRef] [PubMed]
2. Hussam, A. Contending with a development disaster: Sono filters remove arsenic from well water in Bangladesh. *Innovations* **2009**, *4*, 89–102. [CrossRef]
3. Noubactep, C.; Schöner, A.; Woafo, P. Metallic iron filters for universal access to safe drinking water. *Clean Soil Air Water* **2009**, *37*, 930–937. [CrossRef]
4. Noubactep, C. The fundamental mechanism of aqueous contaminant removal by metallic iron. *Water SA* **2010**, *36*, 663–670. [CrossRef]
5. Banerji, T.; Chaudhari, S. A cost-effective technology for arsenic removal: Case study of zerovalent iron-based iit bombay arsenic filter in west bengal. In *Water and Sanitation in the New Millennium*; Nath, K., Sharma, V., Eds.; Springer: New Delhi, India, 2017.
6. Noubactep, C. Editorial for the Special Issue: Filters in Drinking Water Treatment. *Water* **2019**, *11*, 522. [CrossRef]
7. Gonzalez-Perez, A.; Persson, K.M.; Lipnizki, F. Functional channel membranes for drinking water production. *Water* **2018**, *10*, 859. [CrossRef]
8. Hering, J.G.; Maag, S.; Schnoor, J.L. A call for synthesis of water research to achieve the sustainable development goals by 2030. *Environ. Sci. Technol.* **2016**, *50*, 6122–6123. [CrossRef]
9. Noubactep, C.; Licha, T.; Scott, T.B.; Fall, M.; Sauter, M. Exploring the influence of operational parameters on the reactivity of elemental iron materials. *J. Hazard. Mater.* **2009**, *172*, 943–951. [CrossRef]
10. Hu, R.; Gwenzi, G.; Sipowo, R.; Noubactep, C. Water treatment using metallic iron: A tutorial review. *Processes* **2019**, *7*, 622. [CrossRef]

11. Ngai, T.K.K.; Murcott, S.; Shrestha, R.R.; Dangol, B.; Maharjan, M. Development and dissemination of Kanchan™ Arsenic Filter in rural Nepal. *Water Sci. Technol. Water Supply* **2006**, *6*, 137–146. [CrossRef]

12. Naseri, E.; Ndé-Tchoupé, A.I.; Mwakabona, H.T.; Nanseu-Njiki, C.P.; Noubactep, C.; Njau, K.N.; Wydra, K.D. Making Fe⁰-based filters a universal solution for safe drinking water provision. *Sustainability* **2017**, *9*, 1224. [CrossRef]

13. Polonski, M.; Pawluk, K.; Rybka, I. Optimization model for the design of multi-layered permeable reactive barriers. *IOP Conf. Ser. Mater. Sci. Eng.* **2017**, *245*, 072017. [CrossRef]

14. Domga, R.; Togue-Kamga, F.; Noubactep, C.; Tchatchueng, J.B. Discussing porosity loss of Fe⁰ packed water filters at ground level. *Chem. Eng. J.* **2015**, *263*, 127–134. [CrossRef]

15. Makota, S.; Nde-Tchoupe, A.I.; Mwakabona, H.T.; Tepong-Tsindé, R.; Noubactep, C.; Nassi, A.; Njau, K.N. Metallic iron for water treatment: Leaving the valley of confusion. *Appl. Water Sci.* **2017**, *7*, 4177–4196. [CrossRef]

16. Pawluk, K.; Polonski, M.; Wrzesiński, G.; Lendo-Siwicka, M. Two-objective optimization for optimal design of the multilayered permeable reactive barriers. *IOP Conf. Ser. Mater. Sci. Eng.* **2019**, *471*, 112044. [CrossRef]

17. Higgins, M.R.; Olson, T.M. Life-cycle case study comparison of permeable reactive barrier versus pump-and-treat remediation. *Environ. Sci. Technol.* **2009**, *43*, 9432–9438. [CrossRef]

18. Nanseu-Njiki, C.P.; Gwenzi, W.; Pengou, M.; Rahman, M.A.; Noubactep, C. Fe⁰/H₂O filtration systems for decentralized safe drinking water: Where to from here? *Water* **2019**, *11*, 429. [CrossRef]

19. Mwakabona, H.T.; Ndé-Tchoupé, A.I.; Njau, K.N.; Noubactep, C.; Wydra, K.D. Metallic iron for safe drinking water provision: Considering a lost knowledge. *Water Res.* **2017**, *117*, 127–142. [CrossRef]

20. Btatkeu-K, B.D.; Miyajima, K.; Noubactep, C.; Caré, S. Testing the suitability of metallic iron for environmental remediation: Discoloration of methylene blue in column studies. *Chem. Eng. J.* **2013**, *215–216*, 959–968. [CrossRef]

21. Hu, R.; Cui, X.; Xiao, M.; Qiu, P.; Lufingo, M.; Gwenzi, W.; Noubactep, C. Characterizing the suitability of granular Fe⁰ for the water treatment industry. *Processes* **2019**, *7*, 652. [CrossRef]

22. Li, J.; Dou, X.; Qin, H.; Sun, Y.; Yin, D.; Guan, X. Characterization methods of zerovalent iron for water treatment and remediation. *Water Res.* **2019**, *148*, 70–85. [CrossRef] [PubMed]

23. Williamson, S.J.; Clark, L.A. Pressure required to cause cover cracking of concrete due to reinforcement corrosion. *Mag. Concr. Res.* **2000**, *52*, 455–467. [CrossRef]

24. Caré, S.; Nguyen, Q.T.; L'Hostis, V.; Berthaud, Y. Mechanical properties of the rust layer induced by impressed current method in reinforced mortar. *Cement Concr. Res.* **2008**, *38*, 1079–1091. [CrossRef]

25. Zhao, Y.; Yu, J.; Jin, W. Damage analysis and cracking model of reinforced concrete structures with rebar corrosion. *Corros. Sci.* **2011**, *53*, 3388–3397. [CrossRef]

26. Pilling, N.B.; Bedworth, R.E. The oxidation of metals at high temperatures. *J. Inst. Met.* **1923**, *29*, 529–591.

27. Caré, S.; Crane, R.; Calabrò, P.S.; Ghauch, A.; Temgoua, E.; Noubactep, C. Modeling the permeability loss of metallic iron water filtration systems. *Clean Soil Air Water* **2013**, *41*, 275–282. [CrossRef]

28. Moraci, N.; Lelo, D.; Bilardi, S.; Calabrò, P.S. Modelling long-term hydraulic conductivity behaviour of zero valent iron column tests for permeable reactive barrier design. *Can. Geotech. J.* **2016**, *53*, 946–961. [CrossRef]

29. Ndé-Tchoupé, A.I.; Lufingo, M.; Hu, R.; Gwenzi, W.; Ntwampe, S.K.O.; Noubactep, C.; Njau, K.N. Avoiding the use of exhausted drinking water filters: A filter-clock based on rusting iron. *Water* **2018**, *10*, 591. [CrossRef]

30. Noubactep, C. Metallic iron for environmental remediation: Prospects and limitations. In *A Handbook of Environmental Toxicology: Human Disorders and Ecotoxicology*; D'Mello, J.P.F., Ed.; CAB International: Wallingford, UK, 2019; Chapter 36; pp. 531–544.

31. Miyajima, K. Optimizing the design of metallic iron filters for water treatment. *Freib. Online Geosci.* **2012**, *32*, 1–60.

32. Miyajima, K.; Noubactep, C. Characterizing the impact of sand addition on the efficiency of granular iron for water treatment. *Chem. Eng. J.* **2013**, *262*, 891–896. [CrossRef]

33. Li, J.; Zhang, X.; Liu, M.; Pan, B.; Zhang, W.; Shi, W.; Guan, X. Enhanced reactivity and electron selectivity of sulfidated zerovalent iron toward chromate under aerobic conditions. *Environ. Sci. Technol.* **2018**, *52*, 2988–2997. [CrossRef] [PubMed]

34. Gheju, M.; Balcu, I. Removal of chromium from Cr(VI) polluted wastewaters by reduction with scrap iron and subsequent precipitation of resulted cations. *J. Hazard. Mater.* **2011**, *196*, 131–138. [CrossRef] [PubMed]

35. Gheju, M. Progress in understanding the mechanism of Cr^{VI} Removal in Fe^0-based filtration systems. *Water* **2018**, *10*, 651. [CrossRef]

36. Gheju, M.; Balcu, I. Sustaining the efficiency of the Fe^0/H$_2$O system for Cr(VI) removal by MnO$_2$ amendment. *Chemosphere* **2019**, *214*, 389–398. [CrossRef] [PubMed]

37. Sato, N. An overview on the passivity of metals. *Corros. Sci.* **1990**, *31*, 1–19. [CrossRef]

38. Sato, N. Surface oxides affecting metallic corrosion. *Corros. Rev.* **2001**, *19*, 253–272. [CrossRef]

39. Phukan, M. Characterizing the Fe^0/sand system by the extent of dye discoloration. *Freib. Online Geosci.* **2015**, *40*, 1–70.

40. Phukan, M.; Noubactep, C.; Licha, T. Characterizing the ion-selective nature of Fe^0-based filters using azo dyes. *Chem. Eng. J.* **2015**, *259*, 481–491. [CrossRef]

41. Phukan, M.; Noubactep, C.; Licha, T. Characterizing the ion-selective nature of Fe^0-based filters using three azo dyes in batch systems. *J. Environ. Chem. Eng.* **2016**, *4*, 65–72. [CrossRef]

42. Reardon, J.E. Anaerobic corrosion of granular iron: Measurement and interpretation of hydrogen evolution rates. *Environ. Sci. Technol.* **1995**, *29*, 2936–2945. [CrossRef]

43. Landis, R.L.; Gillham, R.W.; Reardon, E.J.; Fagan, R.; Focht, R.M.; Vogan, J.L. An examination of zero-valent iron sources used in permeable reactive barriers. In Proceedings of the 3rd International Containment Technology Conference, Orlando, FL, USA, 10–13 June 2001; Florida State University: Tallahassee, FL, USA, 2001.

44. Miehr, R.; Tratnyek, P.G.; Bandstra, Z.J.; Scherer, M.M.; Alowitz, J.M.; Bylaska, J.E. Diversity of contaminant reduction reactions by zerovalent iron: Role of the reductate. *Environ. Sci. Technol.* **2004**, *38*, 139–147. [CrossRef] [PubMed]

45. Noubactep, C.; Meinrath, G.; Dietrich, P.; Sauter, M.; Merkel, B.J. Testing the suitability of zerovalent iron materials for reactive walls. *Environ. Chem.* **2005**, *2*, 71–76. [CrossRef]

46. Reardon, E.J. Zerovalent irons: Styles of corrosion and inorganic control on hydrogen pressure buildup. *Environ. Sci. Tchnol.* **2005**, *39*, 7311–7317. [CrossRef] [PubMed]

47. Kim, H.; Yang, H.; Kim, J. Standardization of the reducing power of zero-valent iron using iodine. *J. Environ. Sci. Health. A* **2014**, *49*, 514–523. [CrossRef] [PubMed]

48. Birke, V.; Schuett, C.; Burmeier, H.; Friedrich, H.-J. Impact of trace elements and impurities in technical zero-valent iron brands on reductive dechlorination of chlorinated ethenes in groundwater. In *Permeable Reactive Barrier Sustainable Groundwater Remediation*; Naidu, R., Birke, V., Eds.; CRC Press: Boca Raton, FL, USA, 2015; pp. 87–98. ISBN 978-1-4822-2447-4.

49. Li, S.; Ding, Y.; Wang, W.; Lei, H. A facile method for determining the Fe^0 content and reactivity of zero valent iron. *Anal. Methods* **2016**, *8*, 1239–1248. [CrossRef]

50. Pierce, E.M.; Wellman, D.M.; Lodge, A.M.; Rodriguez, E.A. Experimental determination of the dissolution kinetics of zero-valent iron in the presence of organic complexants. *Environ. Chem.* **2007**, *4*, 260–270. [CrossRef]

51. Hildebrant, B. Characterizing the reactivity of commercial steel wool for water treatment. *Freib. Online Geosci.* **2018**, *53*, 1–80.

52. Hu, R.; Ndé-Tchoupé, A.I.; Lufingo, M.; Xiao, M.; Nassi, A.; Noubactep, C.; Njau, K.N. The impact of selected pre-treatment procedures on iron dissolution from metallic iron specimens used in water treatment. *Sustainability* **2019**, *11*, 671. [CrossRef]

53. Ibanez, J.G.; Gonzalez, I.; Cardenas, M.A.J. The effect of complex formation upon the redox potentials of metallic ions: Cyclic voltammetry experiments. *J. Chem. Educ.* **1988**, *65*, 173–175. [CrossRef]

54. Rizvi, M.A.; Syed, R.M.; Khan, B. Complexation effect on redox potential of iron(III)−iron(II) couple: A simple potentiometric experiment. *J. Chem. Educ.* **2011**, *88*, 220–222. [CrossRef]

55. Rizvi, M.A. Complexation modulated redox behavior of transition metal systems. *Russ. J. Gen. Chem.* **2015**, *85*, 959–973. [CrossRef]

56. Bashir, S.; Rizwan, M.S.; Salam, A.; Fu, Q.; Zhu, J.; Shaaban, M.; Hu, H. Cadmium immobilization potential of rice straw-derived biochar, zeolite and rock phosphate: Extraction techniques and adsorption mechanism. *Bull. Environ. Contam. Toxicol.* **2018**, *100*, 727–732. [CrossRef] [PubMed]

57. Sakai, K. Determination of Trace Elements in Steel Using the Agilent 7900 ICP-MS. Agilent Publications 5991-6116EN. 2015. Available online: https://www.agilent.com/cs/library/applications/5991-6116EN-appnote_7900_ICP-MS_steel_analysis.pdf (accessed on 11 October 2018).

58. Zhou, H.; He, Y.; Lan, Y.; Mao, J.; Chen, S. Influence of complex reagents on removal of chromium(VI) by zero-valent iron. *Chemosphere* **2008**, *72*, 870–874. [CrossRef] [PubMed]

59. Elmagirbi, A.; Sulistyarti, H.; Atikah, A. Study of ascorbic acid as iron(III) reducing agent for spectrophotometric iron speciation. *J. Pure App. Chem. Res.* **2012**, *1*, 11–17. [CrossRef]

60. Lufingo, M. Investigation of Metallic Iron for Water Defluoridation. Master's Thesis, Nelson Mandela African Institution of Science and Technology, Arusha, Tanzania, 2019.

61. Noubactep, C.; Caré, S. Dimensioning metallic iron beds for efficient contaminant removal. *Chem. Eng. J.* **2010**, *163*, 454–460. [CrossRef]

62. Noubactep, C. Research on metallic iron for environmental remediation: Stopping growing sloppy science. *Chemosphere* **2016**, *153*, 528–530. [CrossRef] [PubMed]

63. Tarvainen, V.; Ranta-Maunus, A.; Hanhijärvi, A.; Forsén, H. The effect of drying and storage conditions on case hardening of scots pine and norway spruce timber. *Maderas Ciencia y tecnología* **2006**, *8*, 3–14. [CrossRef]

64. Fernando, W.J.N.; Ahmad, A.L.; Shukor, S.R.; Lok, Y.H. A model for constant temperature drying rates of case hardened slices of papaya and garlic. *J. Food Eng.* **2008**, *88*, 229–238. [CrossRef]

65. Noubactep, C.; Caré, S.; Crane, R. Nanoscale metallic iron for environmental remediation: Prospects and limitations. *Water Air Soil Pollut.* **2012**, *223*, 1363–1382. [CrossRef]

66. Huang, C.P.; Wang, H.W.; Chiu, P.C. Nitrate reduction by metallic iron. *Water Res.* **1998**, *32*, 2257–2264. [CrossRef]

67. Hao, Z.-W.; Xu, X.-H.; Wand, D.-H. Reductive denitrification of nitrate by scrap iron filings. *J. Zhejiang Univ. Sci. B* **2005**, *6*, 182–186. [CrossRef] [PubMed]

68. Noubactep, C. Untersuchungen Zur Passiven In. Situ-Immobilisierung von U (VI) aus Wasser. Ph.D. Thesis, Institut für Geologie Freiberg, Freiberg, Germany, 2003.

69. Btatkeu-K, B.D.; Tchatchueng, J.B.; Noubactep, C.; Caré, S. Designing metallic iron based water filters: Light from methylene blue discoloration. *J. Environ. Manag.* **2016**, *166*, 567–573. [CrossRef] [PubMed]

70. Matheson, L.J.; Tratnyek, P.G. Reductive dehalogenation of chlorinated methanes by iron metal. *Environ. Sci. Technol.* **1994**, *28*, 2045–2053. [CrossRef] [PubMed]

71. Liang, L.; Yang, W.; Guan, X.; Li, J.; Xu, Z.; Wu, J.; Huang, Y.; Zhang, X. Kinetics and mechanisms of pH-dependent selenite removal by zero valent iron. *Water Res.* **2013**, *47*, 5846–5855. [CrossRef] [PubMed]

72. Guan, X.; Sun, Y.; Qin, H.; Li, J.; Lo, I.M.C.; He, D.; Dong, H. The limitations of applying zero-valent iron technology in contaminants sequestration and the corresponding countermeasures: The development in zero-valent iron technology in the last two decades (1994–2014). *Water Res.* **2015**, *75*, 224–248. [CrossRef] [PubMed]

73. Noubactep, C. Metallic iron for environmental remediation: A review of reviews. *Water Res.* **2015**, *85*, 114–123. [CrossRef] [PubMed]

74. Ebelle, T.C.; Makota, S.; Tepong-Tsindé, R.; Nassi, A.; Noubactep, C. Metallic iron and the dialogue of the deaf. *Fresenius Environ. Bull.* **2019**, *28*, 8331–8340.

75. Hu, R.; Noubactep, C. Redirecting research on Fe^0 for environmental remediation: The search for synergy. *Int. J. Environ. Res. Public Health* **2019**, *16*, 4465. [CrossRef]

76. Noubactep, C. The operating mode of Fe^0/H_2O systems: Hidden truth or repeated nonsense? *Fresenius Environ. Bull.* **2019**, *28*, 8328–8330.